Supporting Information

Local stabilization of subunit-subunit contacts causes global destabilization of Hepatitis B virus capsids

Christopher John Schlicksup,[1] Patrick Laughlin,[1] Steven Dunkelbarger,[1] Joseph Che-Yen Wang,[1,2] Adam Zlotnick[1*]

1. Molecular and Cellular Biology Department, Indiana University-Bloomington, Bloomington, IN 47401

2. Department of Microbiology and Immunology, Pennsylvania State University College of Medicine, Hershey, PA 17033

* Corresponding Author

Adam Zlotnick

Molecular and Cellular Biology Department

Indiana University-Bloomington

Bloomington, IN 47401

azlotnic@iu.edu

812-856-1925

Keywords: self-assembly, antivirals, Hepatitis B virus, focused reconstruction

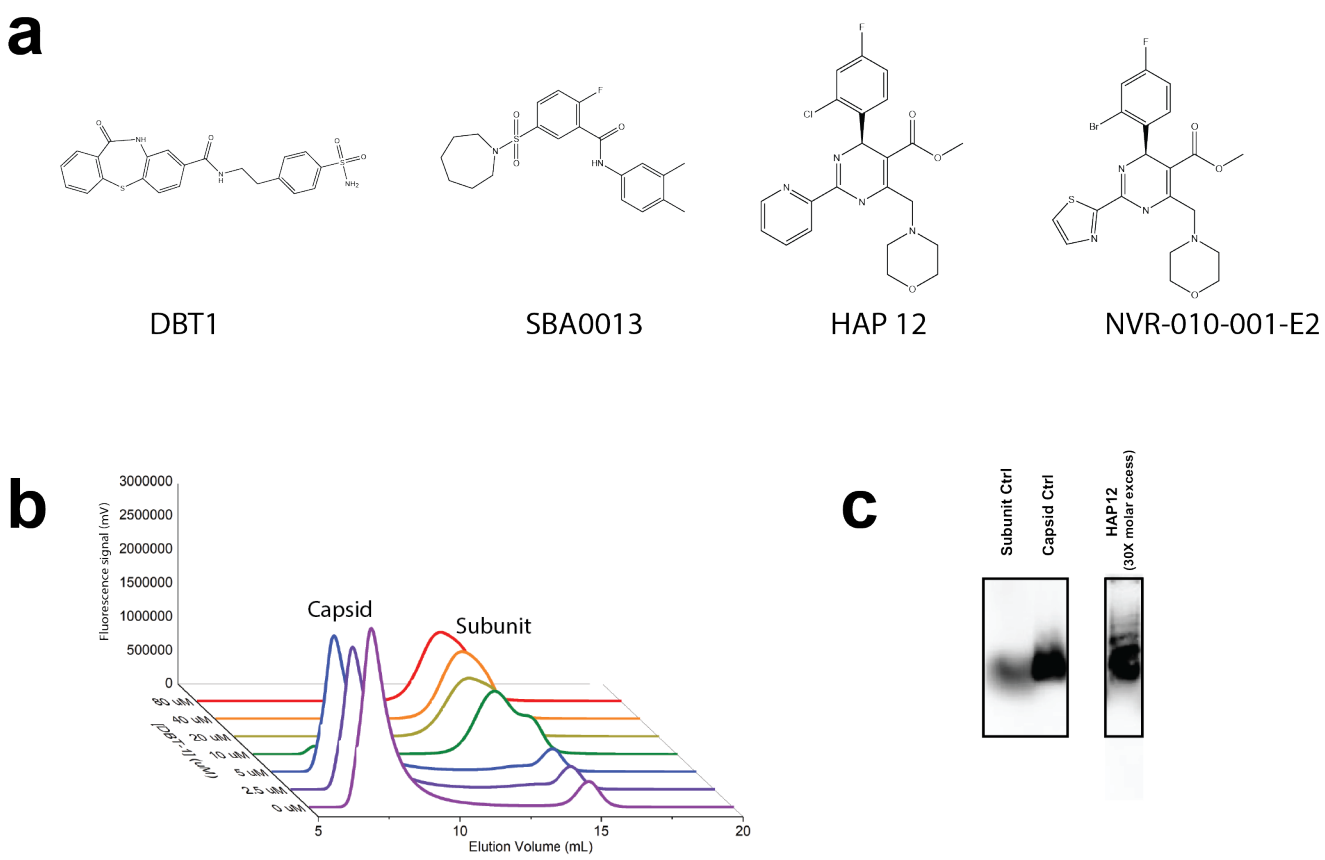

Figure S1. Supplemental chemical structures, size exclusion chromatography, and agarose gel.

(a) Each of the chemical structures used experimentally (DBT1, SBA0013, and HAP12) along with the HAP molecule NVR-010-001-E2, which derives from the high-resolution crystal structure 5E0I, and was used for the molecular docking in (**Fig. 4).** Panel **(b)** uses SEC to recapitulate our observations from the agarose gel electrophoresis in **(Fig. 2a,b),** that DBT1 causes capsids to transition to free subunit. Using shorter running times for the SEC did not detect an increasing dimer pool, consistent with the EM results in **(Fig. 2d).** For us this makes a compelling kinetic argument, that the broken capsid state only exists transiently when treated with DBT1. To further emphasize the disruptive effects of HAP12 on pre-formed capsids, we include another agarose gel blot **(c)**. Here the agarose gel percentage was higher (1.2%) than in **Fig. 2a** (1%), and the distribution of larger mis-assembled products becomes visible. However, the resolution between subunit and capsid become poor, so we opted for the lower agarose condition (1%) for subsequent experiments.

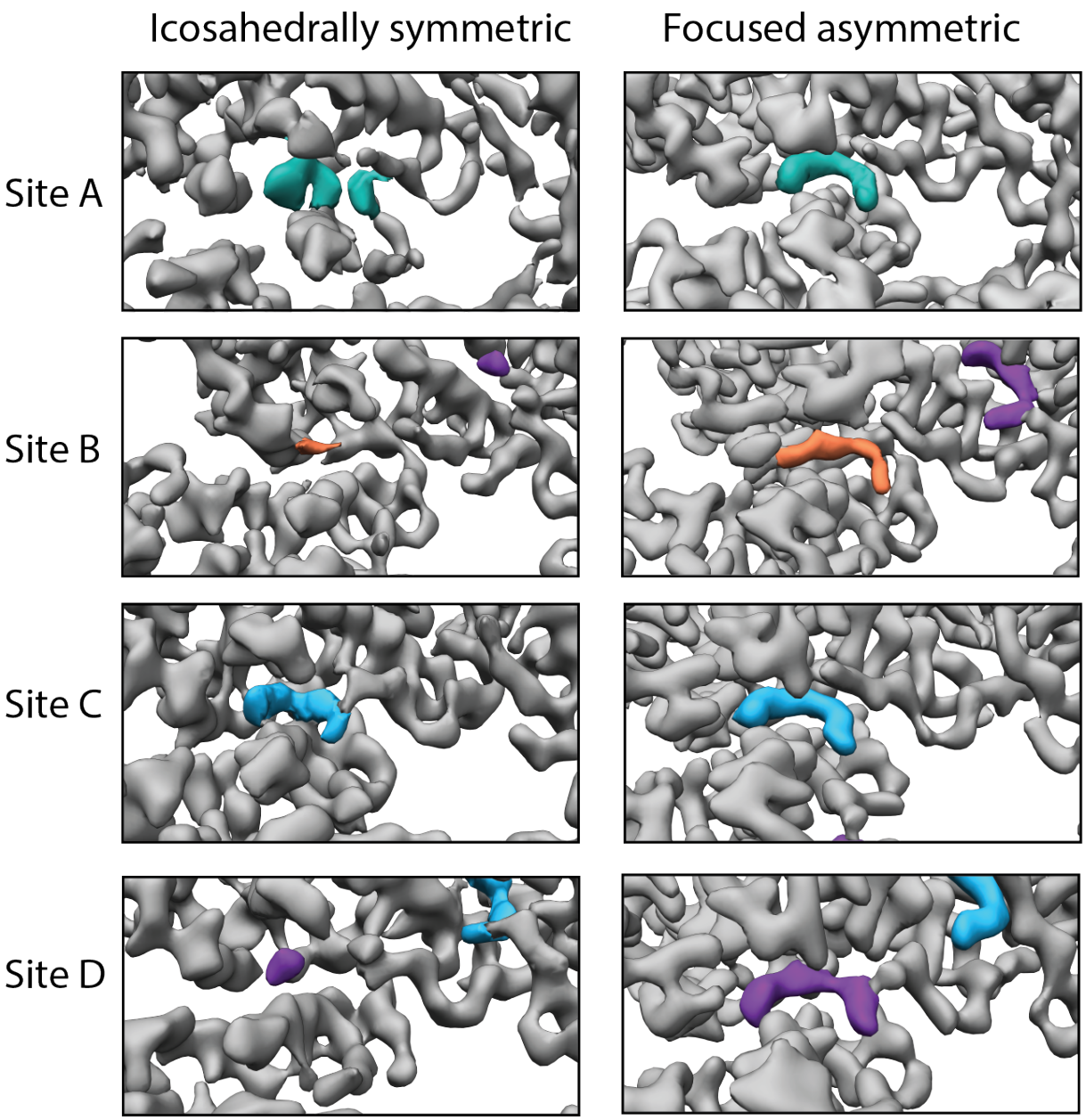

Figure S2. Focused reconstruction reveals detail unseen when imposing icosahedral symmetry. Colored in green is the density in the CpAM pocket. Our initial reconstruction, imposing icosahedral symmetry, had weak and incoherent density for the DBT1 molecule **(left column)**. An alternative reconstruction approach, focused asymmetric reconstruction **(right column),** does not assume perfect capsid symmetry, and dramatically improves the assignment of DBT1 drug density. We interpret the gained clarity to structural variability, both inherent to the capsids and variability imposed by the DBT1-induced strain. By performing focused asymmetric reconstruction, structural variability within a single particle can be individually classified and refined.

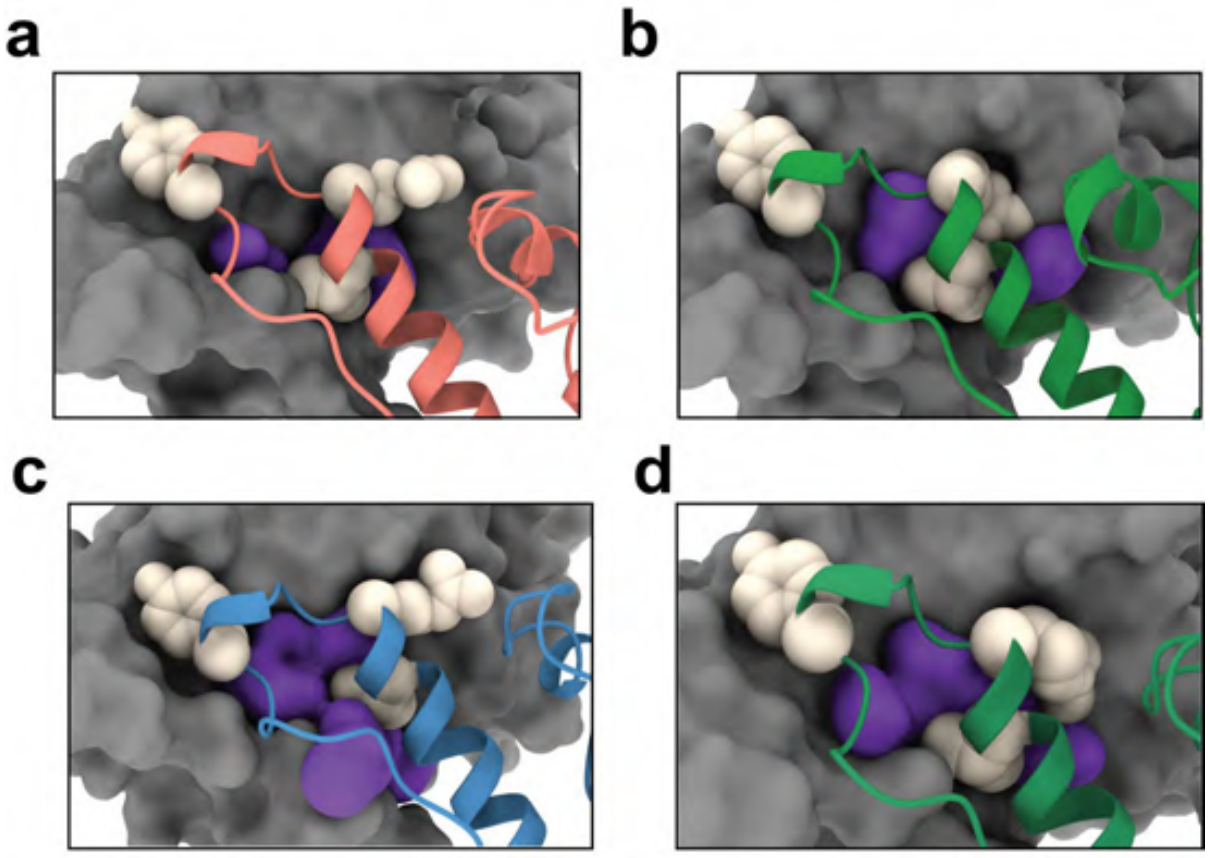

Figure S3. Quasi-equivalence and interface volume. A view of each of the four quasi-equivalent interfaces on the T=4 apo cryo-EM structure (3j2v). Void space is rendered as a purple surface, with important interface residues shown in white (Y132, R127, V124). Despite being composed of identical protein surfaces, each interface is slightly different. This demonstrates the principle of quasi-equivalence and explains how CpAM molecules might bind each interface in a different manner. Interface A **(a)** has basically zero available space in the apo structure. For DBT to bind this site necessitates allosteric changes in quaternary structure (See **Fig. S4).** Site D **(b)** is also quite restrictive, and neither of these sites have been observed to bind HAPs. In comparison, sites B **(c)** and C **(d)** have considerably more accessible volume in the apo capsid, which offers one explanation for how HAPs can bind to these sites.

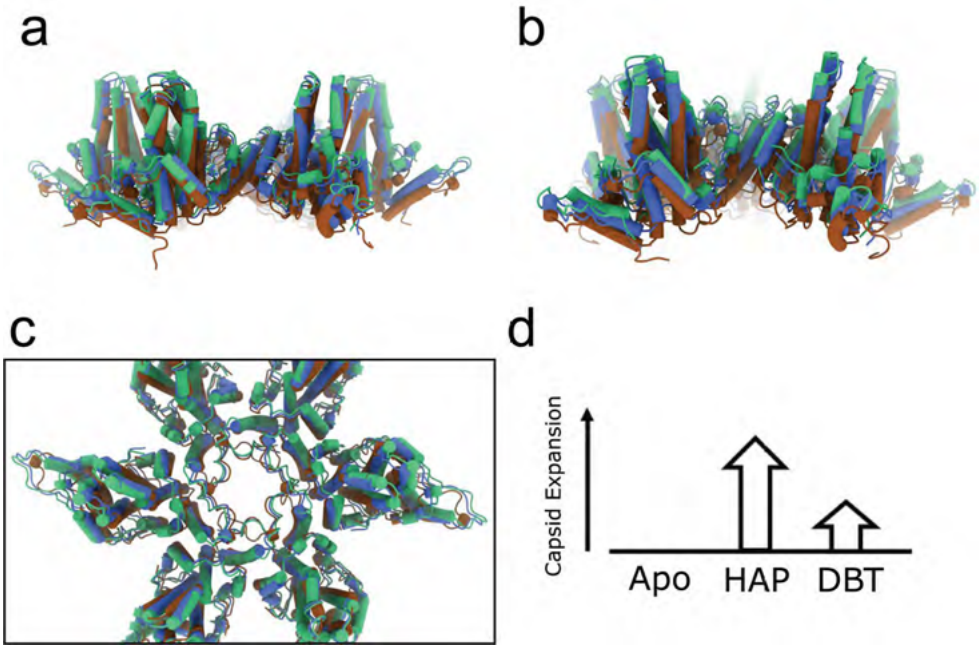

Figure S4. Changes in quaternary structure upon DBT binding. The DBT model (blue) is compared to two references: apo capsid (3J2V, brown) and HAP bound (6BVf, green). Side views of the hexamer **(a)** and pentamer **(b)** demonstrate the variation in capsid diameter between the three structures. Similarly, conclusions are drawn from a top view of the hexamer **(c)**: the structures are similar but contain differences in quaternary structure. Because of the oligomeric nature of the capsid surface, these differences become amplified the further away one compares from the point of alignment. Here the point of alignment is the center of the capsid, thereby equalizing structural differences across the capsid. A schematic of the change in capsid expansion is shown in **(d)**, where the DBT causes a return towards the apo form relative to the HAP bound capsid, despite containing more drug molecules.

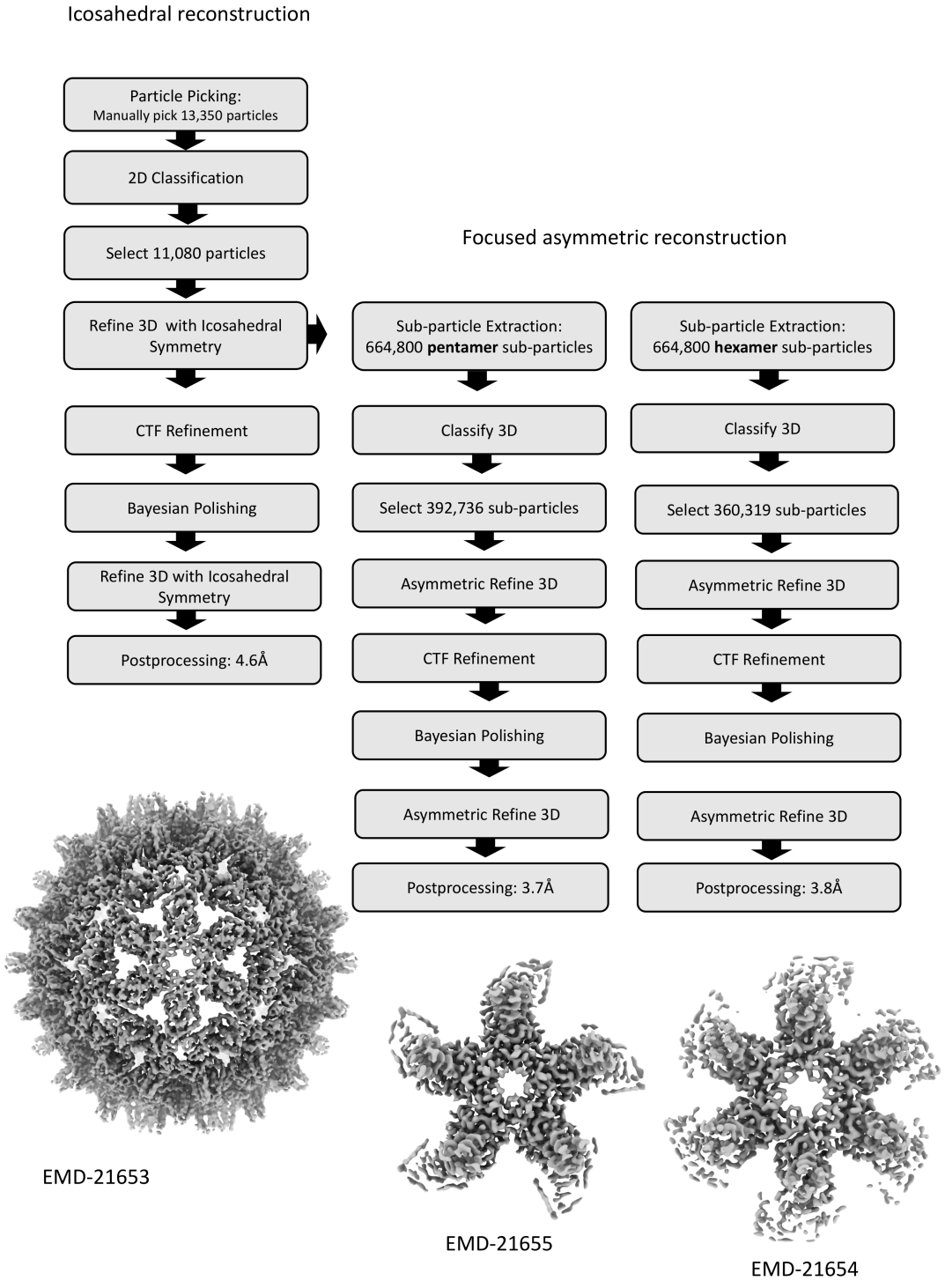

Figure S5. Cryo-EM reconstruction details. A flowchart **(a)** outlines the reconstruction process we used for the cryo-EM image reconstruction. All major steps were performed using Relion 3.0.

Data Collection	
Microscope	FEI Titan Krios
Voltage (kV)	300
Dose (e^- / Å^2)	33
Detector	Gatan K2 Summit
Pixel size (Å)	0.65
Defocus range (μm)	0.5-3.5
Micrographs	680

Density Reconstruction	**Icosahedral**	**Pentamer sub-particle**	**Hexamer sub-particle**
Particle number (Initial)	13,350	-	-
Particle number (Final)	11,080	392,736*	360,319*
Symmetry	Icosahedral	Asymmetric	Asymmetric
Box size (pixels)	640	240	240
Pixel spacing (Å/px)	0.65	0.65	0.65
Sharpening B-factor	-245.503	-212.381	-149.916
Final Resolution	4.6Å	3.7Å	3.8Å
EMDB accession code	EMD-21653	EMD-21655	EMD-21654
PDB accession code	6wfs	6wfs	6wfs

Table S1. Cryo-EM statistics and accession codes. *Particle numbers for the focused asymmetric reconstructions represent subparticles, resulting from expansion of an icosahedral reconstruction using the program *relion_particle_symmetry_expand*.